Electronic Supplementary Material (ESI) for Nanoscale.

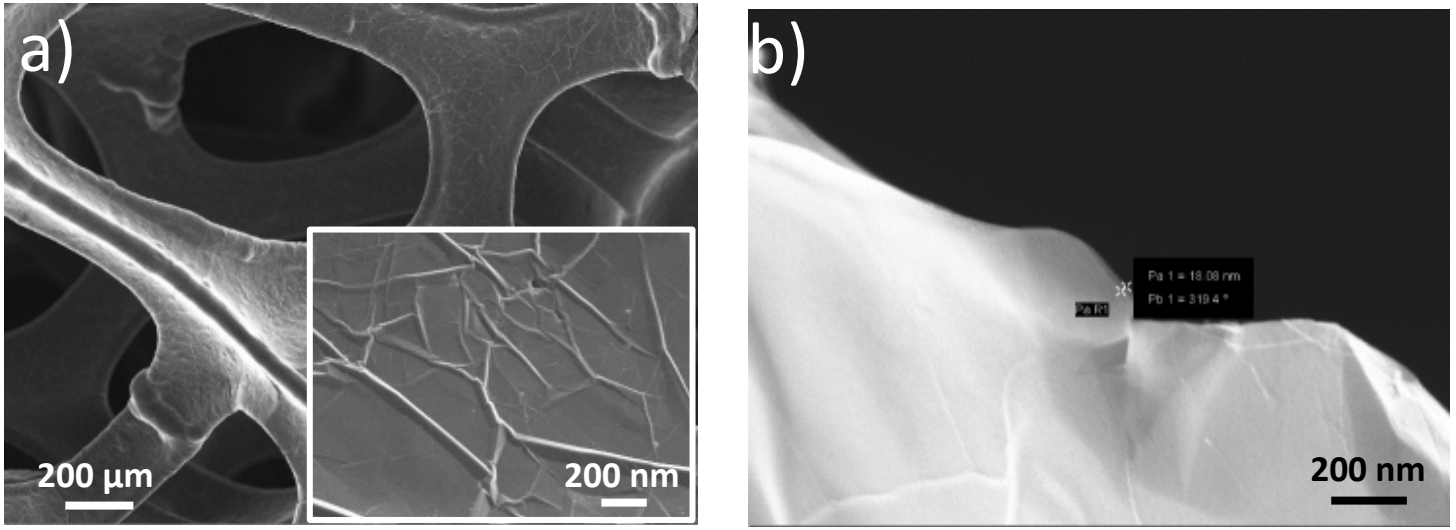

Figure S1. SEM images of bare CVD-Graphene Foam.

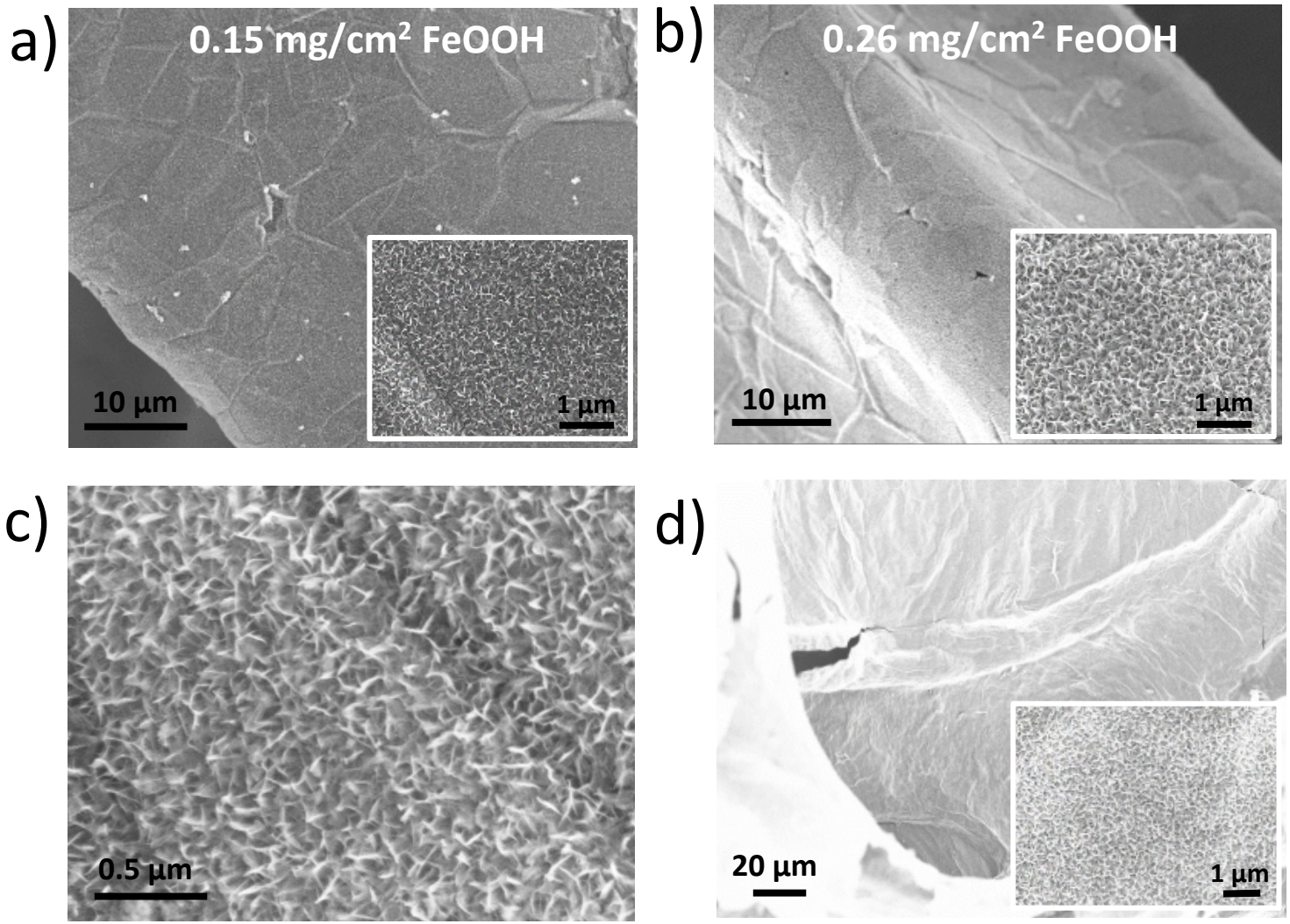

Figure S2. a,b) SEM images of CVD-GF with different loading amount of FeOOH. c) SEM of the Fe_2O_3-GF composite formed after thermal annealing; d) SEM image of FeOOH-EGO-FeOOH-GF, after electrochemical deposition of FeOOH on EGO-FeOOH-GF.

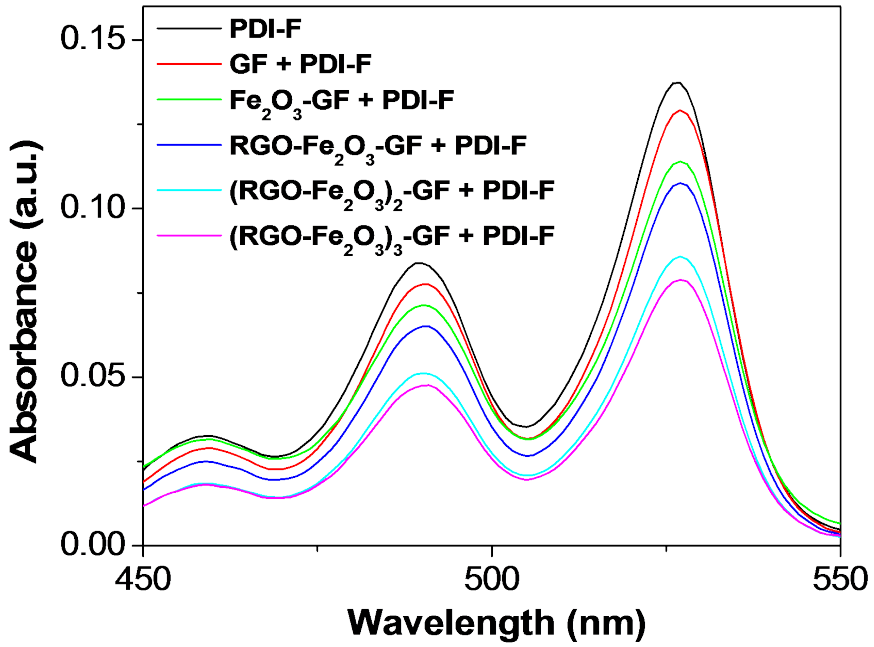

Figure S3. UV-Vis absorption of PDI-F after 7 days' exposure to different GF samples, for surface area measurement.

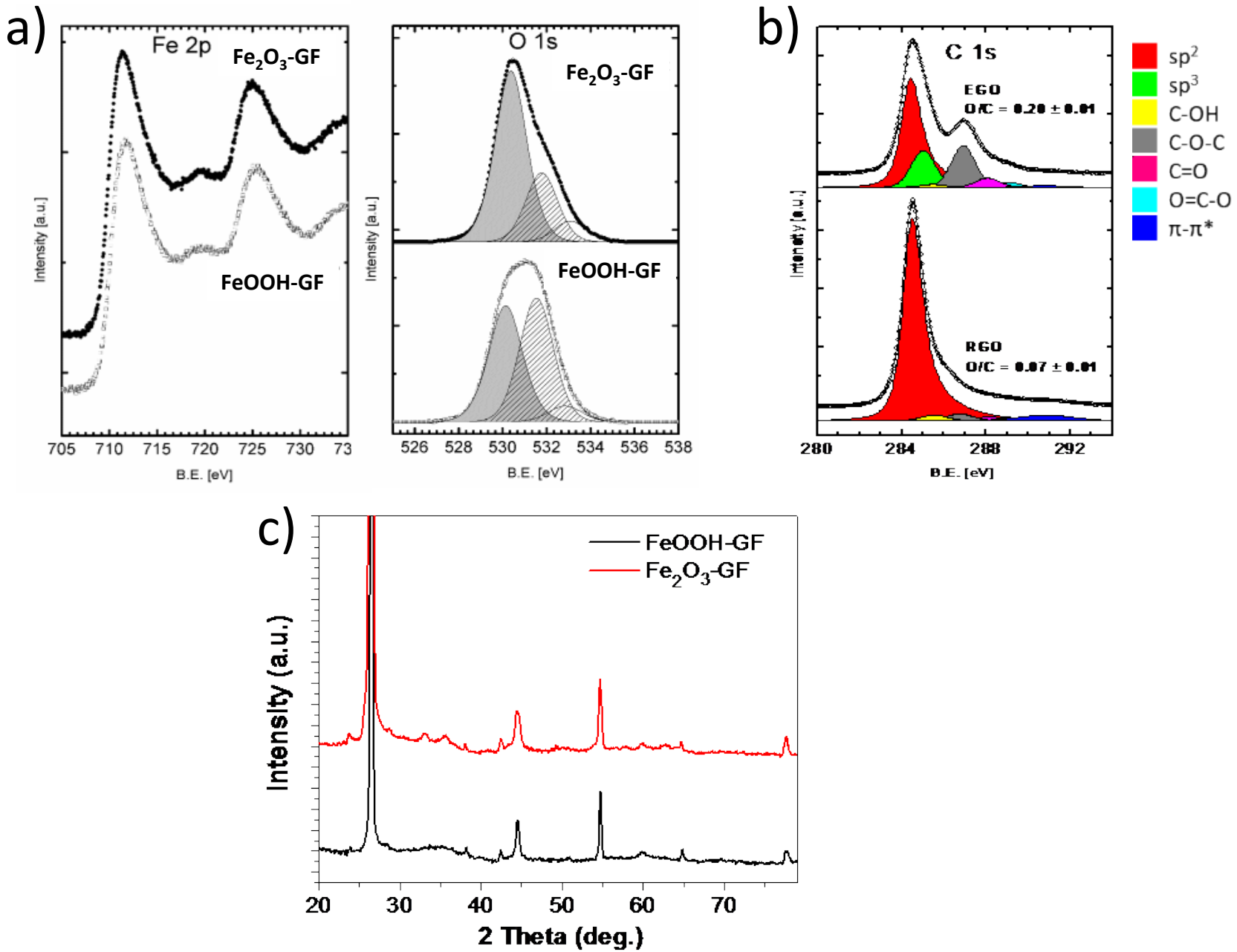

Figure S4. a) XPS spectrum of Fe 2p and O 1s observed in FeOOH-GF and Fe_2O_3-GF composites; b) XPS C 1s peak of pristine EGO and after thermal annealing at 400°C (RGO); c) XRD patterns of the of FeOOH-GF and Fe_2O_3-GF composites.

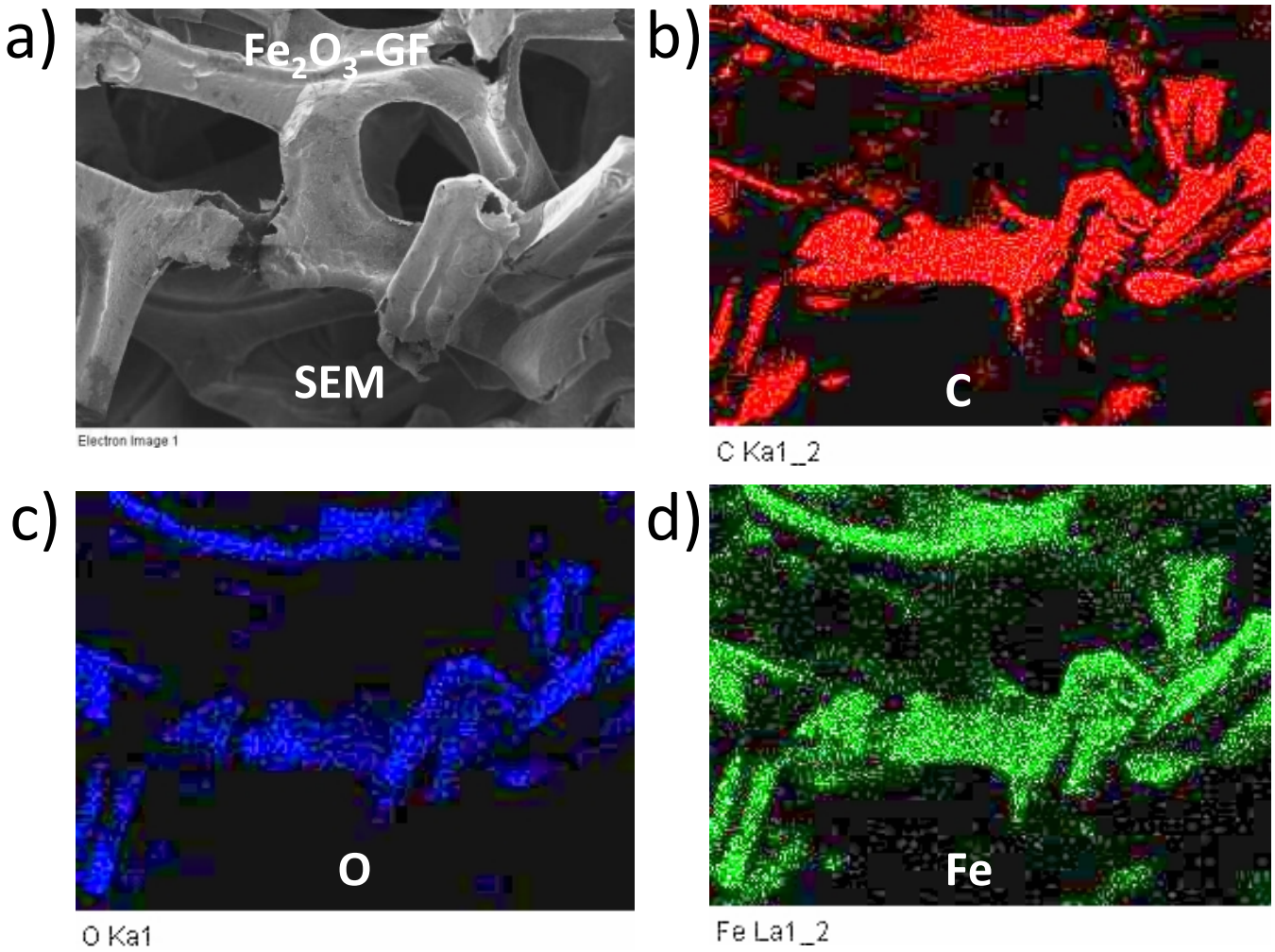

Figure S5. EDS elemental mapping images of the Fe_2O_3-GF composites.

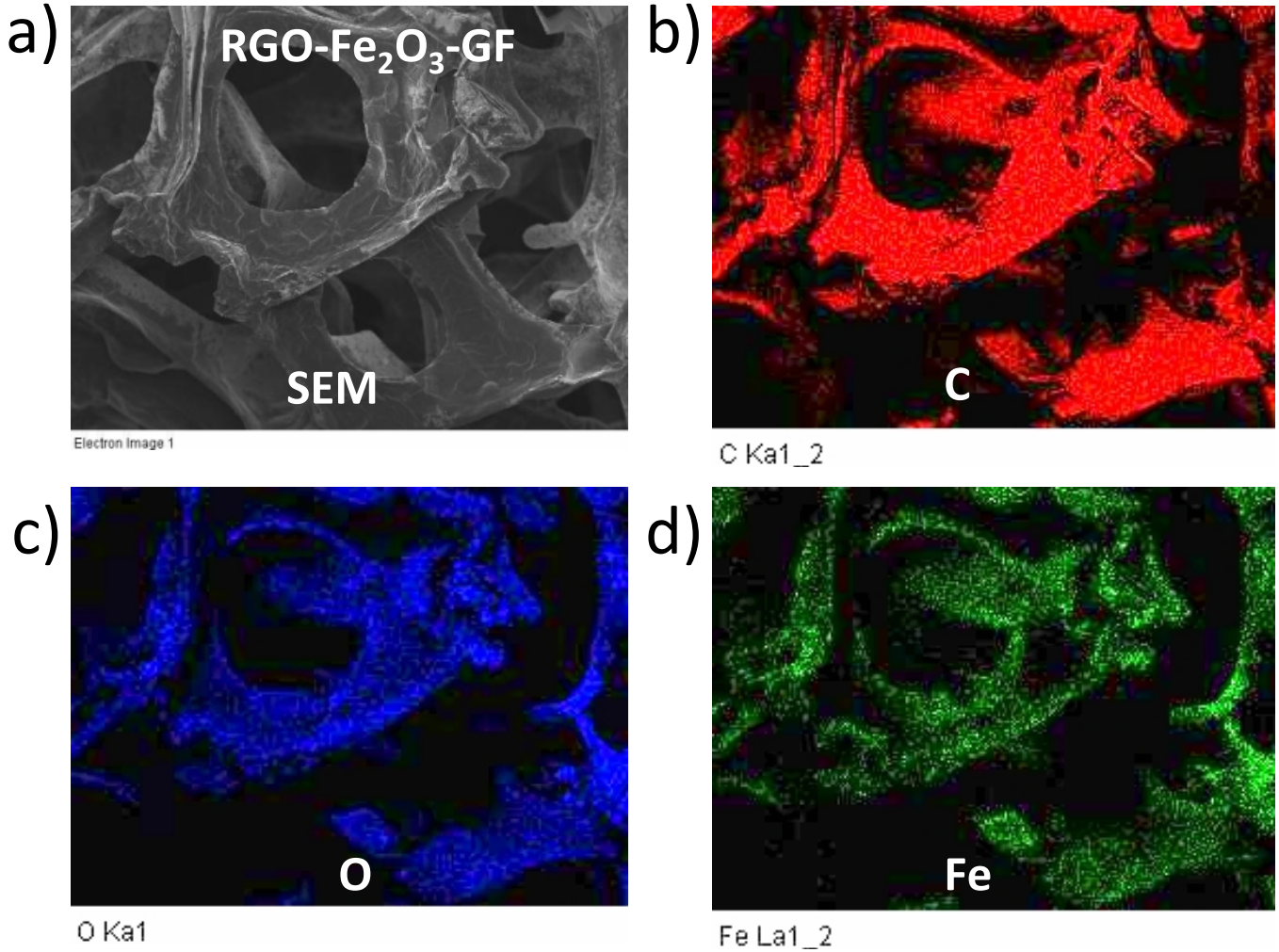

Figure S6. EDS elemental mapping images of the RGO-Fe_2O_3-GF composites.

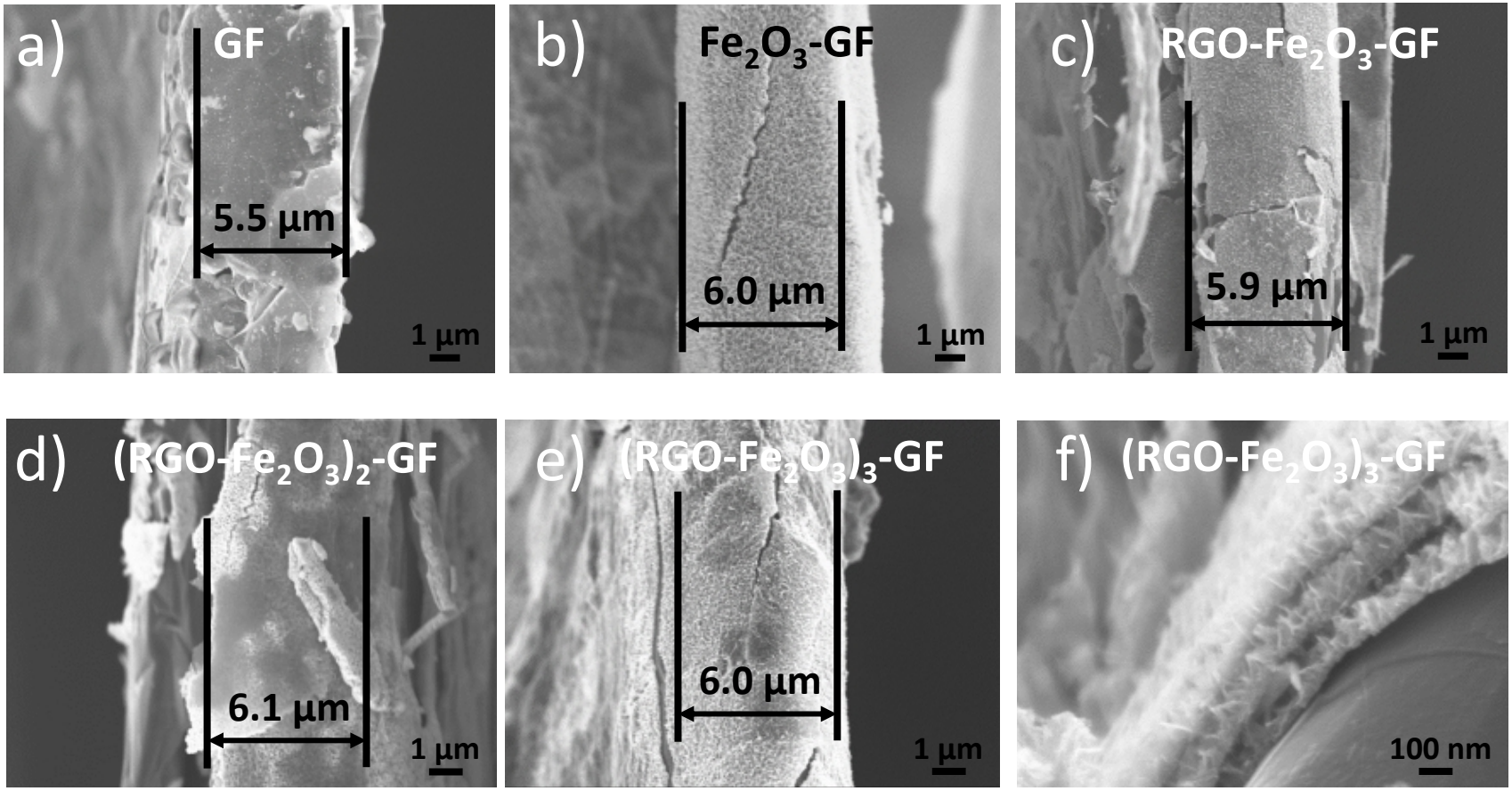

Figure S7. SEM images of GF after compression before testing in batteries: a) bare GF, b) Fe_2O_3-GF, c) RGO-Fe_2O_3-GF, d) (RGO-Fe_2O_3)$_2$-GF, e) (RGO-Fe_2O_3)$_3$-GF; f) cross-section part of the multiple layer Fe_2O_3 coating on (RGO-Fe_2O_3)$_3$-GF surface (also shown in main text).

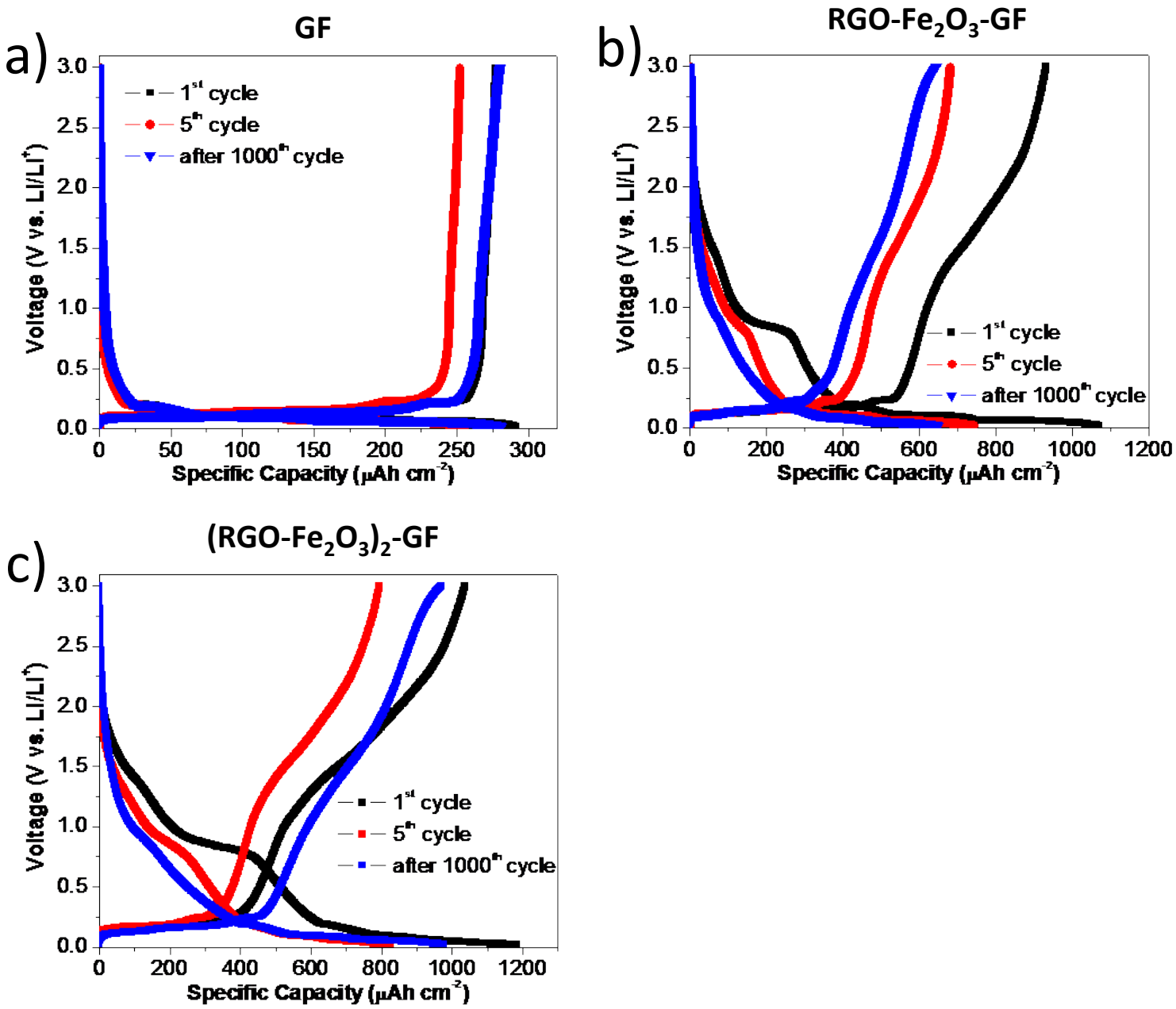

Figure S8. Charge-discharge voltage profiles of a) GF, b) RGO-Fe_2O_3-GF and c) (RGO-Fe_2O_3)$_2$-GF electrodes at 0.2 C

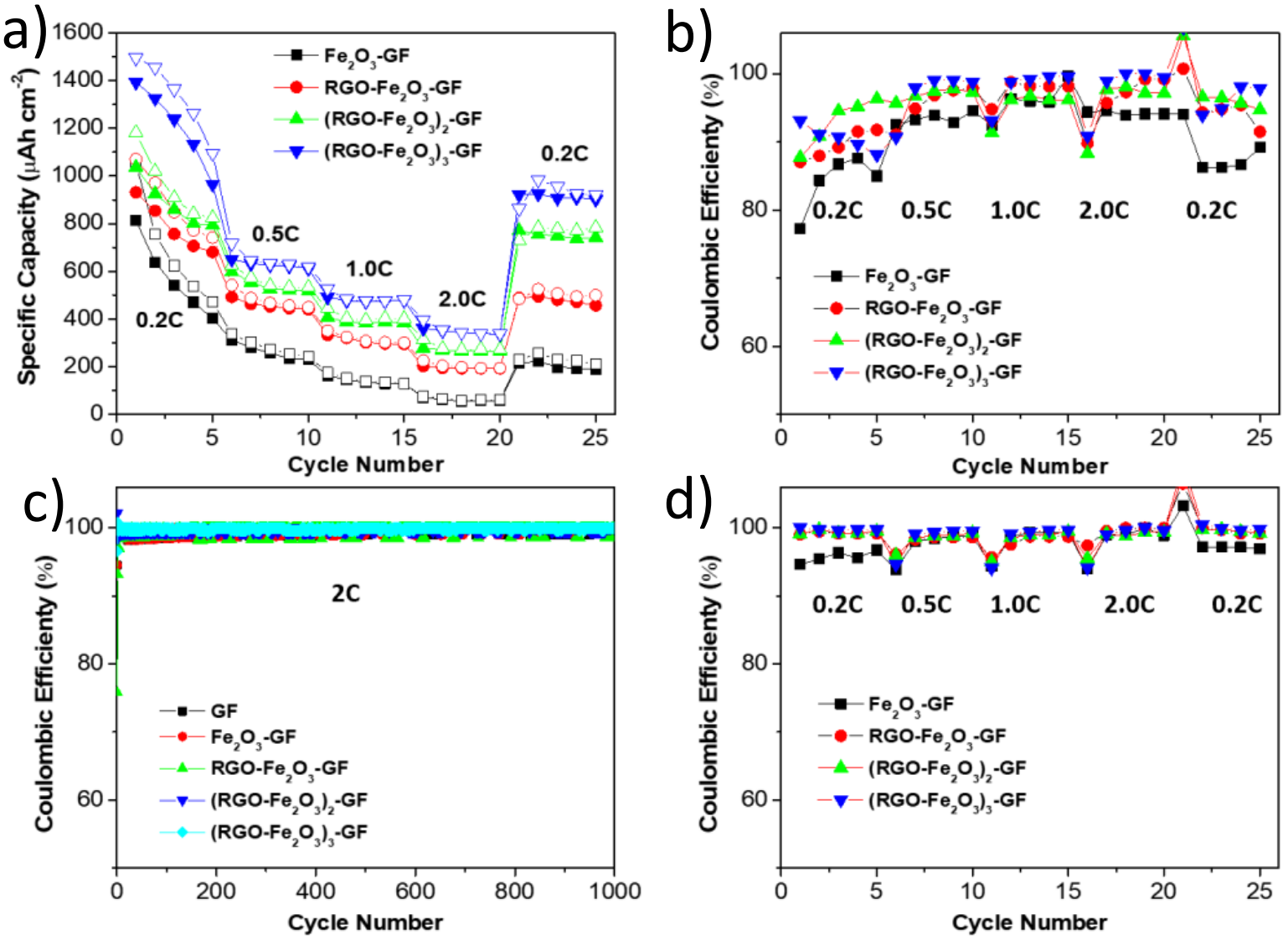

Figure S9. a) Rate capability of the Fe_2O_3 and RGO-Fe_2O_3 based GF composites as anode materials in lithium ion batteries at different discharge and charge rates; Coulombic efficiency of the electrodes b) during the initial 25 cycles at various C rate, c) during the long-term cycles at 2 C, and d) after long-term 1000 cycles at various C rate.

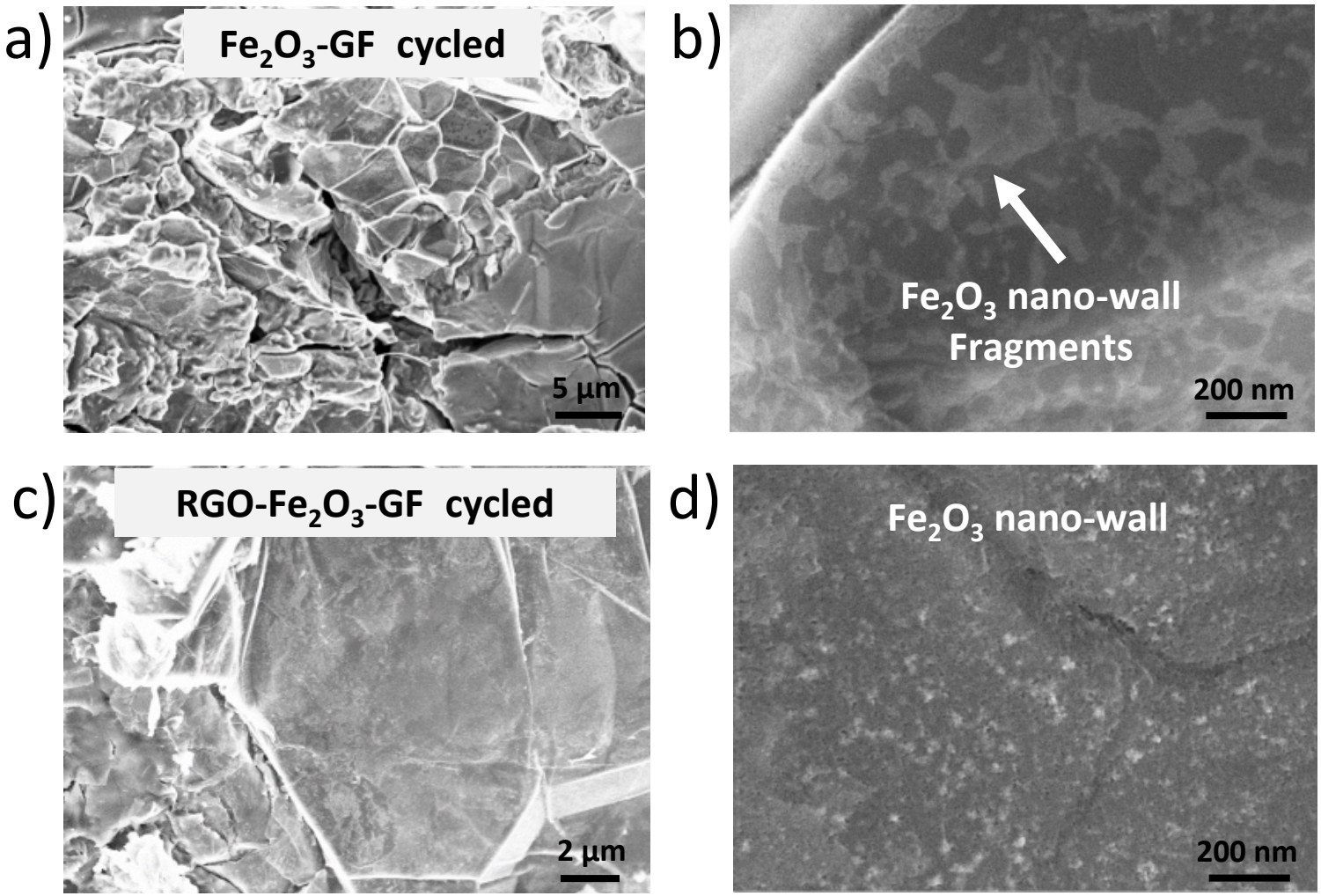

Figure S10. a,b) SEM images of uncoated Fe_2O_3-GF electrodes after 1000 charge/discharge cycles, showing major removal of the Fe_2O_3 layer. c,d) SEM of the RGO-Fe_2O_3-GF composites after 1000 charge/discharge cycles, showing that the nano-wall structure is maintained .

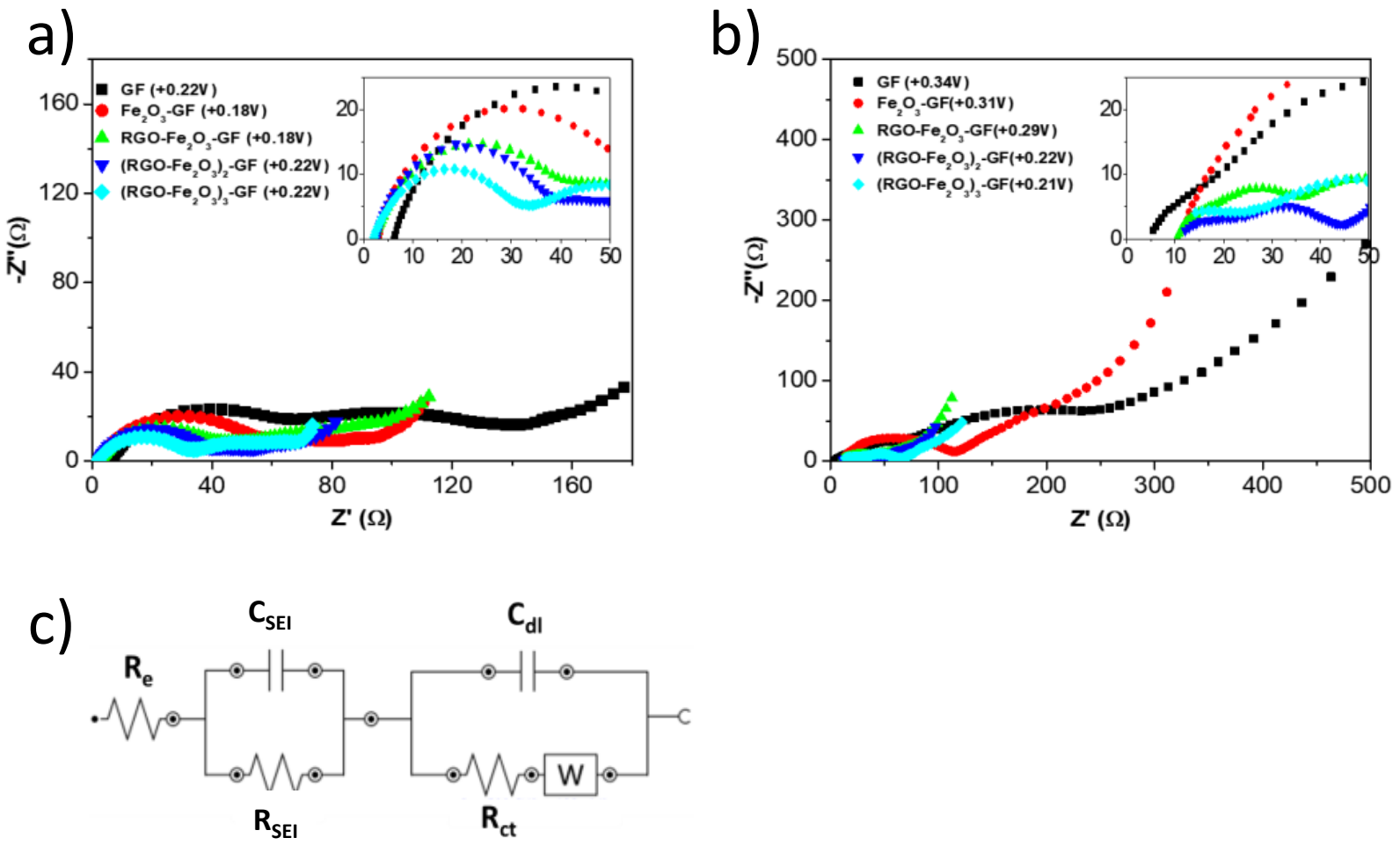

Figure S11. Nyquist impedance plots of the as-assembled bare GF, Fe_2O_3 and RGO-Fe_2O_3 coated GF composites a) before and b) after cycles, the shown EIS were recorded at the open circuit potential; c) Equivalent circuit for the EIS of these electrodes.

Table S1. UV absorption data of GF related composites.

SAMPLE	Absorbance @ 527 (nm)	Concentration (mol/L)	Molecules adsorbed (N^o/g)	Surface Area (m^2/g)
PDI-F original	0.1373	1.73E-06		
GF	0.1292	1.63E-06	1.12E+18	2.34
Fe_2O_3-GF	0.1140	1.43E-06	2.71E+18	5.70
RGO-Fe_2O_3-GF	0.1076	1.35E-06	3.46E+18	7.27
(RGO-Fe_2O_3)$_2$-GF	0.0858	1.08E-06	5.20E+18	10.92
(RGO-Fe_2O_3)$_3$-GF	0.0789	9.93E-07	5.53E+18	11.61

Table S2. Mass contribution of the entire electrodes and the components

Sample	Mass of electrode (mg)	Mass of Fe_2O_3 (mg)	Mass of RGO (mg)	Mass of GF (mg)
GF	1.10	0	0.00	1.10
Fe_2O_3-GF	1.37	0.18	0.00	1.19
RGO-Fe_2O_3-GF	1.38	0.18	0.05	1.15
$(RGO\text{-}Fe_2O_3)_2$-GF	1.59	0.39	0.10	1.10
$(RGO\text{-}Fe_2O_3)_3$-GF	1.98	0.69	0.15	1.15

Table S3. Correspondences of the C-rates and the applied current densities

C-rate*	Current densities (μA cm^{-2})				
	GF	Fe_2O_3-GF	RGO-Fe_2O_3-GF	(RGO-Fe_2O_3)$_2$-GF	(RGO-Fe_2O_3)$_2$-GF
0.2 C	55	83	83	105	144
0.5 C	137	207	208	263	361
1 C	273	413	417	527	723
2 C	545	827	833	1053	1445

* 1C is a rate determined from the weighted average theoretical capacity of all active materials.